Original Investigations

The T_1 State of p-Nitroaniline and Related Molecules: A CNDO/S Study

Richard W. Bigelow

Xerox Webster Research Center, Webster, New York 14580, U.S.A.

Hans-Joachim Freund and Bernhard Dick

Lehrstuhl für Theoretische Chemie der Universität zu Köln, D-5000 Köln,
Federal Republic of Germany

The nature of the lowest energy triplet state (T_1) of p-nitroaniline (PNA), N,N-dimethyl-p-nitroaniline (DMPNA) and nitrobenzene (NB) is re-examined using the semiempirical CNDO/S-CI method with selected parameter options. The present results indicate that in the case of the *unperturbed* molecules the short-axis polarized $\pi^* \leftarrow n(\pi)$ triplet largely localized at the acceptor end of the molecule may lie lower in energy than the triplet manifold counterpart of the intense intramolecular charge-transfer $D^+ \rightarrow A^-$ singlet excitation. Computations suggest, however, that polar solvents strongly stabilize the PNA and DMPNA $\pi^* \leftarrow \pi$ charge-transfer triplet relative to other excitations, whereas specific solvent hydrogen-bonded interactions stabilize the $\pi^* \leftarrow n(\sigma)$ triplet of NB below those of $\pi^* \leftarrow \pi$ character. These assignments allow a rationalization of phosphorescence lifetime data, $T_n \leftarrow T_1$ absorption measurements and relative photochemical behavior.

Key words: p-nitroaniline – Nitrobenzene – Triplet state – Photo reductions – Quantum Yield – Solvent shifts.

1. Introduction

Simple dipolar chemical species (D^+-Ar-A^-) such as the nitroanilines continue to be the subject of considerable interest from both an experimental and theoretical viewpoint [1–18]. This interest unquestionably stems in part from apparent

---

Offprint requests to R. W. Bigelow.

anomalies observed in the luminescence properties [2–6] and XPS core-level photoionization spectra [9–16], in addition to the unusually large nonlinear second-order optical susceptibilities exhibited by these systems [17–23].

Recently McGlynn and co-workers published a series of experimental work on *ortho*, *meta* and *para* nitroanilines [1–6] and correlated their findings with semiempirical CNDO/S MO results as a means of elucidating the electronic structure as a function of substituent [1, 3–6]. Briefly, McGlynn and co-workers concluded from comparisons between their experimental and computational work [5] that the T_1 state of the p-nitroanilines studied was the triplet counterpart to the $\pi^* \leftarrow \pi$ charge-transfer singlet excitation. It was emphasized that such an assignment was consistent with the polarization of phosphorescence. The computational scheme used by McGlynn and co-workers [4, 5] employed Nishimoto–Mataga (NM) [24] two-center coulomb integrals and yielded several PNA excitations from *localized* oxygen orbitals to the molecular π^*-levels which were ≥ 1.0 eV lower in energy than the best estimates of the corresponding experimental energies: two $\pi^* \leftarrow n(\sigma)$ excitations calculated at 2.90 and 3.05 eV, respectively, in the singlet manifold and a single $\pi^* \leftarrow \pi$ excitation in the triplet manifold calculated at 1.8 eV. Based on reasonable arguments McGlynn and co-workers [4] considered these excitations, at the energies calculated, to be artifacts of the computational method. Consequently, the low-lying $\pi^* \leftarrow \pi$ triplet excitation was excluded from subsequent discussions of the excitation and luminescence properties of PNA and DMPNA [4, 5, 25].

Our CNDO/S-CI analysis on p-nitroaniline and related molecules [8, 15, 16] characterizes this low-lying triplet as derived from a $\pi^* \leftarrow n(\pi)$ transition largely localized at the acceptor end of the molecule with a short-axis polarization, an assignment also noted by McGlynn and co-workers [5] as being consistent with phosphorescence polarization results [26, 27]. While parameters more suitable for the description of triplet properties (Pariser–Parr (PP) [28, 29] two-center coulomb integrals) confirms that the low energy of the $\pi^* \leftarrow n(\pi)$ state in question
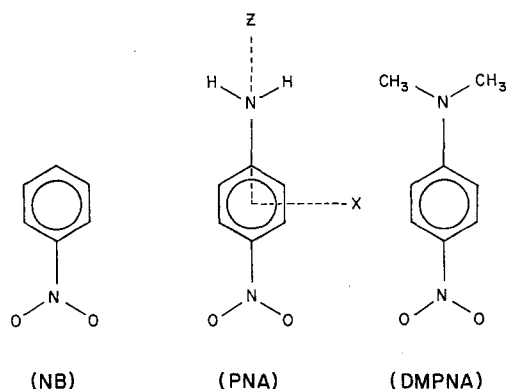

Fig. 1. Molecules considered in this study: nitrobenzene (NB); p-nitroaniline (PNA); and *N,N*-dimethyl-p-nitroaniline (DMPNA)

is indeed an artifact of the computational scheme used by McGlynn and co-workers [4, 5] particularly the NM integral approximation, this state remains below or approximately energetically degenerate with the $D^+ \to A^- \pi^* \leftarrow \pi$ charge-transfer triplet. The purpose of this work, therefore, is to examine the spectroscopic manifestations of a charge-transfer versus a "locally"-excited T_1 state assignment. We loosely define the $\pi^* \leftarrow n(\pi)$ transition in question as "locally"-excited because the NH_2 group is unaffected, although charge density differences indicate considerable charge-transfer from the nitro group to the aromatic ring. The implications of our computational findings on p-nitroaniline (PNA), N,N-dimethyl-p-nitroaniline (DMPNA) and nibrobenzene (NB), Fig. 1, are discussed within the content of phosphorescence lifetime data, $T_n \leftarrow T_1$ absorption measurements and relative photochemical behavior.

2. Computational Procedure

The closed-shell CNDO/S-CI molecular orbital program of DelBene and Jaffé [30] as developed by Ellis, Kuehnlenz and Jaffé [31] for the study of $\pi^* \leftarrow n(\sigma)$ singlet excitations was used. Particular parametrizations are described in the text. Computations involving doubly excited states were carried out as described separately for singlets [32] and triplets [33].

We have noted in previous studies that small variations in molecular geometries relative to experimental values do not significantly perturb the properties of current interest. Atomic coordinates for the molecules considered here were, therefore, taken from our earlier work [8, 15, 16] unless otherwise indicated, in which case the bondlengths and angles are those given by Pople and Beveridge [34].

3. Results and Discussion

3.1. Ordering of Excitations

Numerous computations conducted by us on the isolated molecular systems, Fig. 1, show the relative *ordering of orbitals* to be relatively insensitive to moderate changes in parameters or structure, Fig. 2. Particularly important to our interpretation is the relatively small binding energy difference between the oxygen π-orbital lone-pair and the highest occupied molecular orbital in NB, PNA and DMPNA. The ordering of the three highest occupied orbitals of PNA is in accord with the *ab initio* results of Domcke et al. [13]. Other techniques have been shown to yield some variation in this regard [18, 36], where, for example, the *ab initio* computations of Bertinelli and co-workers [36], place the oxygen π-orbital lone-pair energetically degenerate with the HOMO level. In approximate accord with our results the MINDO/3 technique [37] places the NB oxygen π-orbital lone-pair ~ 1.5 eV below the HOMO level. The present calculated energy differences of the three highest occupied orbitals of NB, PNA and DMPNA using identical parametrizations reflect the experimental variation in the first three photoelectron peak positions as a function of substituent [1].
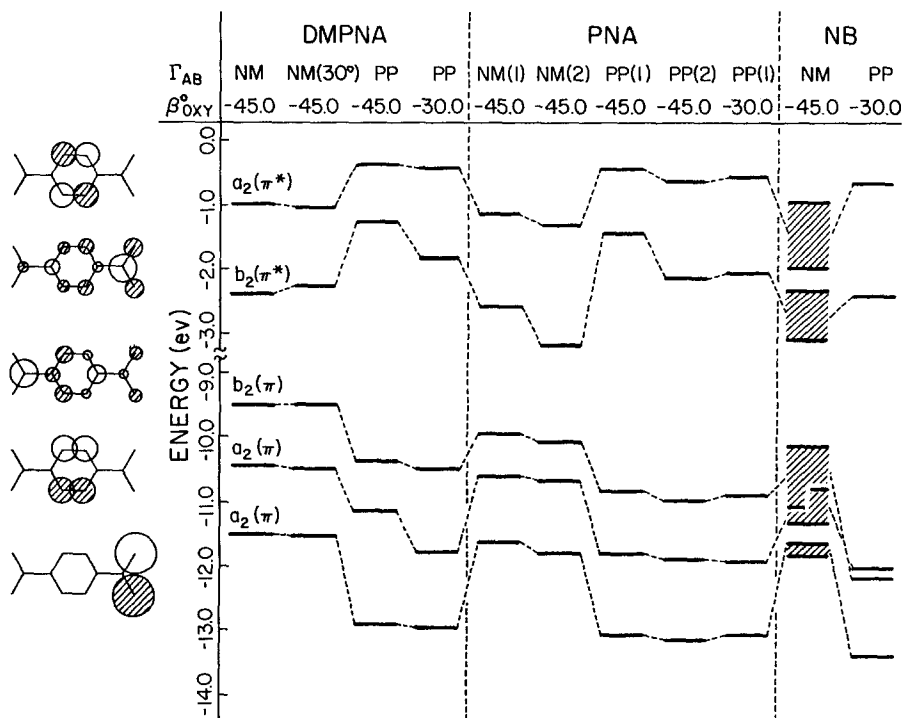
Fig. 2. The calculated ordering and energies of the orbitals of interest. Particular parametrization options used in each case are given in the appropriate column: NM (Nishimoto–Mataga two-center Coulomb integrals); PP (Pariser–Parr two-center integrals); $\beta^0_{OXY} = -45.0$ eV (the original CNDO/S oxygen parameter appearing in the off-diagonal one-electron Fock operator – Ref. [30]; and $\beta^0_{OXY} = -30.0$ eV (the modified oxygen parameter recently developed by Jacques and co-workers for use with the CNDO/S technique – Ref. [35]. The DMPNA results corresponding to $\theta = 30°$ represents a twist of the nitro group 30° out of the ring plane, otherwise all molecules were considered to have a planar π-structure. The results given for NB using NM integrals represents the spread obtained from nine separate calculations of varying aromatic and substituent bondlengths. Characterization (1) and (2) under PNA corresponds to two slightly differing geometries. The schematic orbitals are of DMPNA ($\beta^0_{OXY} = -30.0$ eV; PP integrals) given in C_{2v} symmetry. The orbital lobes are drawn proportional to the AO coefficients and are viewed from above the molecular plane

We have calculated the electronic excitation spectra by means of a configuration interaction treatment including single and double excited configurations. The electron–electron interaction integrals,

$$\Gamma_{AB} = \langle \mu_1 \nu_2 | r_{12}^{-1} | \mu_1 \nu_2 \rangle \tag{1}$$

are approximated in this work by either the NM or PP method. It has been suggested in the literature, with particular emphasis on benzene, that when these approximations are used with the CNDO/S parametrization and configuration interaction is limited to singly-excited states, NM integrals yield better singlet states while the PP approximation is better suited for triplets [38, 39]. Theoretical

arguments attribute these difficulties to relative electron correlation effects which are sensitive to the variation of Γ_{AB} as a function of interatomic distance [40, 41].

Restricting computations to singly-excited states we find that regardless of the integral approximation used the T_1 state of NB, PNA and DMPNA is invariably derived from a one-electron excitation from the oxygen π-orbital lone-pair (Fig. 2) to π^*-levels having considerably large coefficients on the nitro group. The lower-lying triplet state orderings were also found to be insensitive to the number of configurations used to generate the excited states. Our computations on PNA (60×60 CI) using NM integrals gave $T_1 = 1.75$ eV well separated from the $T_2(D^+ \rightarrow A^-)$ intramolecular charge-transfer state at 2.79 eV, whereas $T_1 = 3.01$ eV and $T_2 = 3.34$ eV were obtained using PP integrals. Figure 3 provides
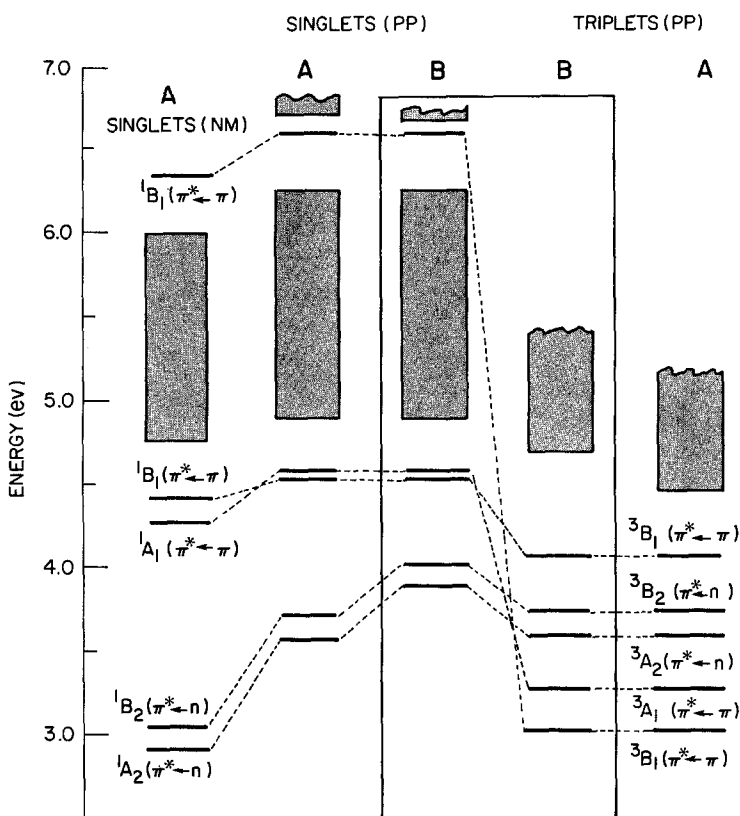

Fig. 3. The correlation diagram of the lower-lying excitations of PNA as described in the text obtained using a 60×60 CI expansion: A-computed and B-adjusted. NM corresponds to Nishimoto–Mataga integrals, whereas PP corresponds to Pariser–Parr integrals. Labels are in terms of C_{2v} symmetry. The hatched areas correspond to regions where additional excitations are calculated to occur. The small exchange splitting of the $B_1(\pi^* \leftarrow \pi)$ excitation just below the hatched areas is due to a dramatically different CI composition of the singlet and triplet components. We were unable to duplicate the $^1B_1(\pi^* \leftarrow \pi)/^1A_1(\pi^* \leftarrow \pi)$ ordering of McGlynn et al. [4, 5] and Smith and co-workers [25] $(E(^1B_1) < E(^2A_1))$ using NM integrals for any reasonable geometry variation

Table 1. The low-lying excitation energies (eV) of NB and DMPNA calculated with PP integrals (C_{2v} symmetry). The $^1A_2$ and $^1B_2$ energies have been adjusted upward in energy by 0.35 eV in accord with arguments in the text

	NB(PP)		DMPNA(PP)	
$^1A_2(\pi^* \leftarrow n(\sigma))$	3.92	$^1A_2(\pi^* \leftarrow n(\sigma))$	4.09	
$^1B_2(\pi^* \leftarrow n(\sigma))$	4.06	$^1B_2(\pi^* \leftarrow n(\sigma))$	4.19	
$^1B_1(\pi^* \leftarrow \pi)$	4.64	$^1A_1(\pi^* \leftarrow \pi)$	4.32	
$^1A_1(\pi^* \leftarrow \pi)$	4.90	$^1B_1(\pi^* \leftarrow \pi)$	4.36	
$^3B_1(\pi^* \leftarrow n(\pi))$	2.88	$^3B_1(\pi^* \leftarrow n(\pi))$	3.00	
$^3A_1(\pi^* \leftarrow \pi)$	3.33	$^3A_1(\pi^* \leftarrow \pi)$	3.11	
$^3A_2(\pi^* \leftarrow n(\sigma))$	3.58	$^3A_2(\pi^* \leftarrow n(\sigma))$	3.74	
$^3B_2(\pi^* \leftarrow n(\sigma))$	3.71	$^3B_2(\pi^* \leftarrow (\sigma))$	3.84	

a correlation of the lower-lying excitations of PNA, whereas corresponding excitations are given for NB and DMPNA in Table 1. Singlet and triplet transitions arising from the same $\pi^* \leftarrow n(\sigma)$ excitation are energetically degenerate in ZDO methods due to the neglect of one-center exchange terms. Both the corresponding singlet and triplet energies are obtained according to the Roothaan [42] prescription for the triplet manifold resulting in a calculated singlet excitation too low in energy by twice the exchange interaction. The $\pi^* \leftarrow n(\sigma)$ singlet excitations have, therefore, been adjusted (corrected) upward in energy in accord with the results of preliminary INDO/S calculations [33]. The calculated value (0.35 eV) is in general agreement with the small exchange splitting of $\pi^* \leftarrow n(\sigma)$ excitations found in other systems [43–45]. It is apparent that, in addition to yielding a triplet state manifold more closely approximating experiment than NM integrals (assuming the solvent effects to be discussed below), PP integrals with subsequent adjustments to reflect exchange interactions also shift the $\pi^* \leftarrow (\sigma)$ singlets to the precise energy range suggested by McGlynn and co-workers [4, 5]. In general the experimental values for the T_1 state of NB, PNA and DMPNA obtained in condensed media lie between ~2.29 and 2.62 eV [2, 7, 46] or approximately $0.4 \rightarrow 0.7$ eV below the energy calculated for T_1. It should be noted that while a weak phosphorescence has been detected for NB [46, 47] recent work attributes this emission to impurities [3, 7, 48]. The anomalous character of NB luminescence is addressed in greater detail below.

We performed a cursory examination of the effects on the electronic structure of PNA of including doubly-excited states in the configuration interaction [32, 33]. Briefly, we find relative to corresponding computations using singly-excited states: (1) doubly-excited configurations do not alter the character of the T_1 state; (2) the $T_1 - S_0$ splitting is significantly enhanced in the computation employing NM integrals due to a large selective stabilization of S_0; (3) after configuration interaction including doubly-excited configurations the energy of T_1 is comparable for both NM and PP integral approximations (~$3.2 \rightarrow 3.4$ eV); and (4) the $T_n \leftarrow T_1$ spacings are not greatly modified between π-orbital excitations. Also, the T_1/T_2 ordering in NB is preserved when doubly-excited states
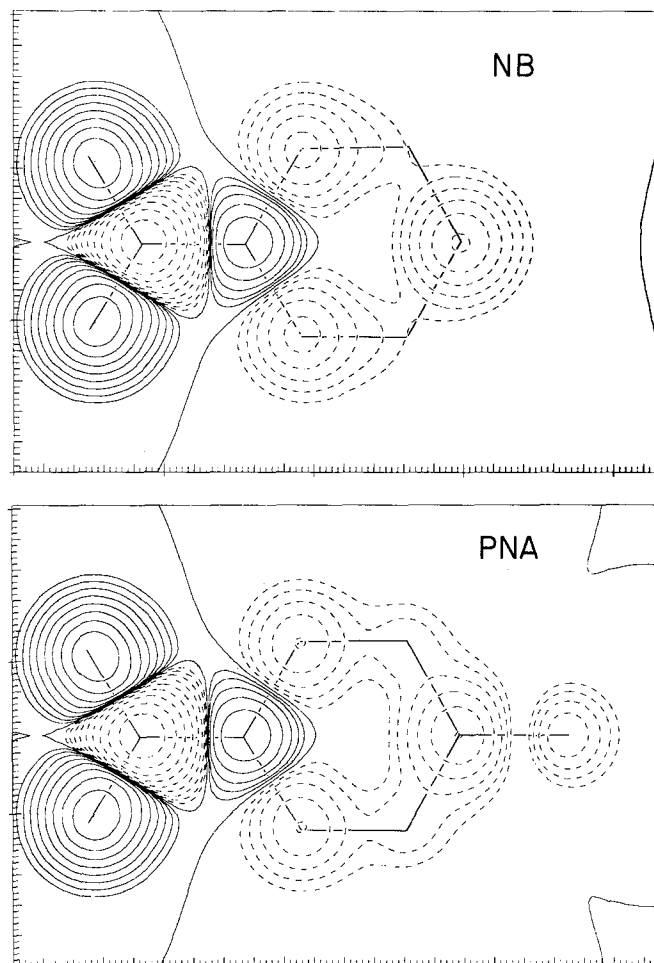
Fig. 4. Electron density difference diagrams for the NB and PNA $1\,^3B_1(\pi^* \leftarrow n(\pi))$ excitation at 1.5 Å above the molecular plane. Solid lines correspond to a positive charge density difference relative to S_0, whereas dashed lines represent a negative charge density difference

are included, whereas these levels are reversed in the case of DMPNA: $T_1 \rightarrow$ 3.22 eV and $T_2 \rightarrow 3.10$ eV. Based on the ordering of the states in Fig. 3 and Table 1 the following discussion assumes the T_1 state of the *unperturbed* molecules to be either $\pi^* \leftarrow \pi(D^- \rightarrow A^+)$ or $\pi^* \leftarrow n(\pi)$ character. Electron-density difference diagrams are presented in Figs. 4 and 5 for the unperturbed T_1 and T_2 states of NB and PNA to emphasize the character of these excitations.

3.2. Phosphorescence (Spin–Orbit Coupling) Mechanisms Appropriate for PNA (DMPNA)

The phosphorescence lifetime of PNA is $0.2 \rightarrow 0.4$ sec. [2, 7] and provides one possible means of establishing the T_1 state character. The emissive lifetime of
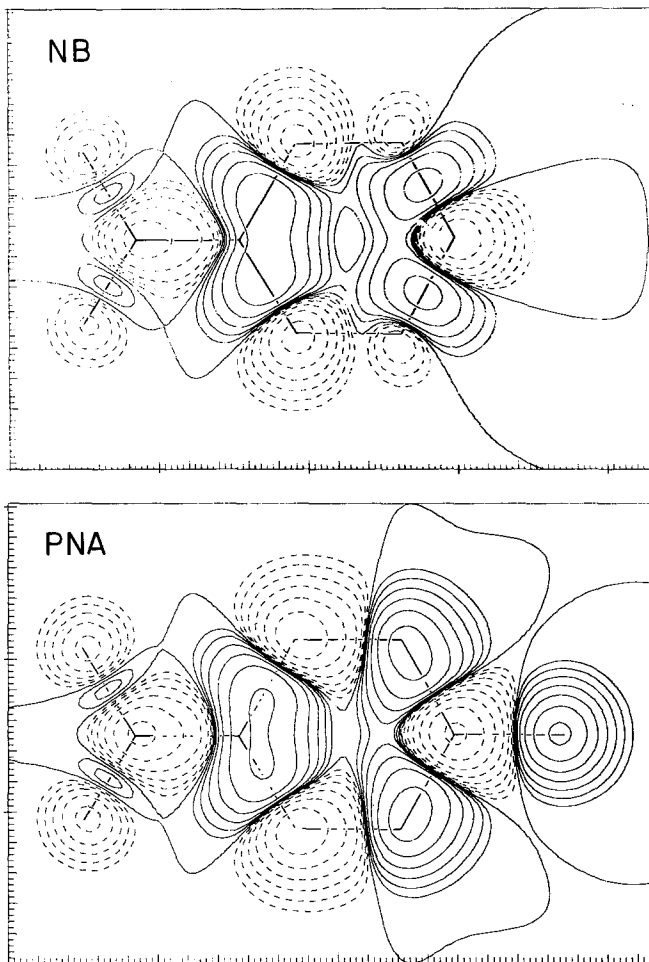
Fig. 5. Electron density difference diagrams for the NB and PNA $1^3A_1(\pi^* \leftarrow \pi)$ excitation at 1.5 Å above the molecular plane. Solid lines correspond to a positive charge density difference relative to S_0, whereas dashed lines represent a negative charge density difference

T_1 is given by [49–51],

$$\frac{1}{\tau_p^0} = \frac{64\pi^4 v^3}{3hc^3} \sum_{m_s} \left| \sum_k \frac{\langle S_k|H'|T_1^{m_s}\rangle}{E(T_1) - E(S_k)} \langle S_0|e\vec{r}|S_k\rangle + \sum_l \frac{\langle T_l^{m_s}|H'|S_0\rangle}{E(S_0) - E(T_l)} \langle T_l^{m_s}|e\vec{r}|T_1^{m_s}\rangle \right|^2$$

(2)

where H' is the one-electron spin–orbit coupling operator defined in terms of the orbital angular momentum, $\vec{l}_i$, and spin angular momentum, $\vec{s}$, operators by [49–51],

$$H' = \sum_i \xi(r_i)\vec{l}_i \cdot \vec{s}_i$$

(3)

The first term in Eq. (2) represents coupling of higher-lying singlet states directly to T_1 (Mechanism I), whereas the second term corresponds to direct interaction of higher-lying triplets with the ground state (Mechanism II). Assuming that T_1 is either the $^3B_1(\pi^* \leftarrow n(\pi))$ or $^3A_1(\pi^* \leftarrow \pi)$ state, symmetry arguments restrict the matrix elements for out-of-plane polarized phosphorescence to [49–51],

$$^3B_1: \quad \begin{array}{ll} \text{I} & \langle S_k(B_2)|H_z'(A_2)|T_1(B_1)\rangle\langle S_0(A_1)|r_y(B_2)|S_k(B_2)\rangle \\ \text{II} & \langle T_l(A_2)|H_z'(A_2)|S_0(A_1)\rangle\langle T_l(A_2)|r_y(B_2)|T_1(B_1)\rangle \end{array}$$

$$^3A_1: \quad \begin{array}{ll} \text{I} & \langle S_k(B_2)|H_x'(B_2)|T_1(A_1)\rangle\langle S_0(A_1)|r_y(B_2)|S_k(B_2)\rangle \\ \text{II} & \langle T_l(B_2)|H_x'(B_2)|S_0(A_1)\rangle\langle T_l(B_2)|r_y(B_2)|T_1(A_1)\rangle \end{array}$$

First, assuming T_1 is the $^3B_1$ state and restricting analysis to the lower-lying excited states in Table 2 it is found that the primary term in Mechanism I is the $S_k(2^1B_2)$ configuration, which leads to the relative contribution,

$$\frac{1}{\tau_p^0} \propto 10^{-5}\langle 22|H'|24\rangle \tag{4}$$

Orbitals $|22\rangle$ and $|24\rangle$ are largely localized on the oxygen atoms and lead to an integral of much greater magnitude than obtained between any other orbital pairs. Although there are several higher-lying excited singlets of appropriate symmetry with $f(S_k \leftarrow S_0)$ typically 10^{-3}–10^{-4}, the relevant spin–orbit coupling terms become vanishingly small due to orbital localizations. According to Table 2 there are no T_l states with $f(T_l \leftarrow T_1) > 2.0 \times 10^{-5}$ and Mechanism II cannot therefore provide terms of comparable magnitude to the leading term in Mechanism I.

Assuming T_1 is the $^3A_1$ state, it is found that the $S_k(13^1B_2)$ state is the largest contributor to Mechanism I,

$$\frac{1}{\tau_p^0} \propto 2.0 \times 10^{-4}\langle 19|H'|26\rangle \tag{5}$$

$|19\rangle$ and $|26\rangle$ are delocalized over the carbon framework which constitutes an efficient route to phosphorescence. Contributions from $S_k(2^1B_2)$ and $S_k(10^1B_2)$ become vanishingly small due to relative orbital localizations. $T_l(25^3B_2) \leftarrow T_1(^3A_1)$ is the only $T_l \leftarrow T_1$ excitation of sufficient oscillator strength to permit Mechanism II to compete with the above route in Mechanism I. The $T_l(25^3B_2)$ state, however, leads to spin–orbit coupling terms involving s-orbital character and $\langle T_l(25^3B_2)|H'|S_0\rangle$ consequently becomes vanishingly small. Expanding the matrix elements in terms of the LCAO wavefunctions, retaining only one-center terms and substituting the spin–orbit coupling parameters of Masmanidis and co-workers [38] ($\zeta(C) = 28$ cm^{-1}, $\zeta(N) = 70$ cm^{-1}, $\zeta(O) = 156$ cm^{-1}) yields $\langle 22|H'|24\rangle/\langle 19|H'|26\rangle \sim 10.0$. It should be emphasized that the *observed* out-of-plane polarized phosphorescence and C_{2v} symmetry excludes SOC contributions from $\pi^* \leftarrow \pi$ singlet states – the strongly dipole allowed $\pi^* \leftarrow \pi$ intramolecular charge-transfer excitation, for example.

Table 2. The PNA excitations (60×60 CI; PP integrals; $\beta^0_{OXY} = -45.0$ eV) used to address spin–orbit coupling and the $T_n \leftarrow T_1$ absorption spectrum. E is the excitation energy relative to the ground state, $\mu(D)$ the excited state dipole moment $- \mu(S_0) = 7.90$ $D(PP)$, E'_{SOL} is the solvation energy calculated according to Jano (Ref. 52) $- E'_{SOL}(S_0) = 2.68$ (PP), and f is the oscillator strength between the indicated configurations. In order to calculate $f[T_i \leftarrow T_1(^3A_1)]$ we performed a supermolecule calculation by placing NH_4^+ opposite the PNA nitro group. This geometry served to selectively stabilize the LUMO NO_2-orbital (Ref. 16) leading to a level reversal of the two lowest triplets of the isolated system. This perturbation causes the slight difference in oscillator strength between the two lowest triplets shown in the table. Other triplet state values are referenced to the free molecule. Excited state dipole moments were calculated for states whose $f(T_i \leftarrow T_1)$ was $\geq 1.0\times10^{-6}$

S_k	E (eV)	$\mu(D)$	E'_{SOL}	$f[S_k \leftarrow S_0]$	Wavefunction
$2\,^1B_2(\pi^* \leftarrow n)$	4.04	6.14	1.09	8.3×10^{-5}	$0.851|22\to27)+0.500|22\to29)+\cdots$
$10\,^1B_2(\pi^* \leftarrow \sigma)$	7.04	6.81	2.60	1.2×10^{-3}	$-0.956|21\to28)+0.253|23\to28)+\cdots$
$13\,^1B_2(\pi^* \leftarrow \sigma)$	7.76	8.78	2.52	1.7×10^{-3}	$0.790|19\to27)+0.343|22\to29)+\cdots$

T_i	E (eV)	$\mu(D)$	E'_{SOL}	$f[T_i \leftarrow T_1(^3B_1)]$	$f[T_i \leftarrow T_1(^3A_1)]$	Wavefunction
$1\,^3B_1(\pi^* \leftarrow \pi)$	3.02	5.05	1.08	—	1.9×10^{-3}	$0.846|24\to27)+0.514|24\to29)+\cdots$
$2\,^3A_1(\pi^* \leftarrow \pi)$	3.34	9.91	3.86	9.0×10^{-4}	—	$0.857|26\to27)-0.354|26\to29)+\cdots$
$3\,^3A_2(\pi^* \leftarrow n)$	3.59	—	1.01	4.0×10^{-6}	—	$0.839|23\to27)+0.494|23\to29)+\cdots$
$4\,^3B_2(\pi^* \leftarrow n)$	3.69	—	1.11	—	7.0×10^{-6}	$0.851|22\to27)+0.500|22\to29)+\cdots$
$8\,^3A_1(\pi^* \leftarrow \pi)$	5.29	13.19	3.35	1.7×10^{-2}	8.5×10^{-2}	$-0.815|26\to29)+0.401|20\to27)+\cdots$

$9\ ^3A_1(\pi^* \leftarrow \pi)$	6.45	13.39	3.70	5.4×10^{-3}	1.0×10^{-1}	$-0.810\lvert26\to30)+0.314\lvert26\to29)+\cdots$
$11\ ^3A_2(\pi^* \leftarrow \sigma)$	6.77	—	3.92	2.1×10^{-5}	—	$-0.918\lvert21\to27)+0.162\lvert23\to27)+\cdots$
$12\ ^3B_2(\pi^* \leftarrow \sigma)$	7.04	—	2.60	—	1.1×10^{-5}	$-0.956\lvert21\to28)+0.253\lvert23\to28)+\cdots$
$14\ ^3B_2(\pi^* \leftarrow \sigma)$	7.76	—	2.52	—	1.7×10^{-5}	$0.792\lvert19\to27)+0.278\lvert22\to27)+\cdots$
$15\ ^3A_2(\pi^* \leftarrow \sigma)$	7.92	—	2.13	1.0×10^{-6}	—	$-0.807\lvert19\to28)+0.504\lvert22\to28)+\cdots$
$16\ ^3B_2(\sigma^* \leftarrow \pi)$	7.98	—	2.46	—	9.9×10^{-4}	$-0.905\lvert26\to31)+0.248\lvert26\to32)+\cdots$
$17\ ^3A_1(\pi^* \leftarrow \pi)$	8.17	14.08	3.62	1.4×10^{-2}	8.3×10^{-1}	$0.814\lvert20\to27)+0.427\lvert26\to30)+\cdots$
$18\ ^3B_2(\pi^* \leftarrow n)$	8.30	—	1.80	—	6.0×10^{-6}	$0.630\lvert23\to28)+0.498\lvert22\to29)+\cdots$
$19\ ^3A_2(\pi^* \leftarrow \sigma)$	8.33	—	1.84	1.5×10^{-5}	—	$0.509\lvert22\to28)+0.506\lvert21\to29)+\cdots$
$20\ ^3B_1(\pi^* \leftarrow \pi)$	8.36	5.02	1.34	1.4×10^{-1}	1.0×10^{-6}	$0.747\lvert24\to29)-0.514\lvert24\to27)+\cdots$
$24\ ^3B_2(\pi^* \leftarrow n)$	8.69	—	1.45	—	6.0×10^{-6}	$-0.525\lvert23\to28)-0.418\lvert22\to29)+\cdots$
$25\ ^3B_2(\sigma^* \leftarrow \pi)$	8.71	—	2.45	—	2.7×10^{-2}	$-0.851\lvert26\to32)+0.341\lvert26\to31)+\cdots$

32 – σ^* delocalized on carbon centers (s-orbitals)
31 – σ^* delocalized on carbon centers (s-orbitals)
30 – π^* delocalized on carbon centers
29 – π^* 40% localized on NO_2 group
28 – π^* delocalized on carbon atoms
27 – π^* 50% localized on NO_2 group
26 – π 24% localized on NH_2 group

25 – π delocalized on carbon centers
24 – $n(\pi)$ localized on oxygen atoms
23 – $n(\sigma)$ localized on oxygen $P\sigma$ orbitals
22 – $n(\sigma)$ localized on oxygen $P\sigma$ orbitals
21 – σ delocalized on carbon $p\sigma$ orbitals
20 – π delocalized on carbon centers
19 – σ delocalized on carbon $p\sigma$ orbitals

Our analysis, therefore, suggests that, although the routes to phosphorescence are significantly different, $^3A_1$ and $^3B_1T_1$ state character is expected to yield "comparable" phosphorescence lifetimes.

3.3. $T_l \leftarrow T_1$ Absorption and Solvent Effects

Wolleben and Testa [7] conclude that the T_1 state of PNA is intramolecular charge-transfer in nature based upon three experimental observations: (1) the $T_l \leftarrow T_1$ absorption maximum of PNA is shifted to longer wavelengths relative to corresponding excitations in benzene and aniline, (2) there is an order of magnitude decrease in the phosphorescence lifetime in going from aniline to PNA, and (3) PNA exhibits negligible photoreduction in isopropyl alcohol relative to nitrobenzene. Observation 1 of Wolleben and Testa, while implying that the resolved $T_l \leftarrow T_1$ absorption involves the substituents, and hence is probably intramolecular charge-transfer in nature, does not, however, explicitly probe the character of the initial state which is T_1: it could as well be a manifestation of the final state. Our computational results, for example, indicate a roughly comparable $T_l \leftarrow T_1$ absorption spectrum for PNA in the wavelength region of interest assuming either $T_1(^3A_1)\,D^+ \leftarrow A^-$ charge-transfer or $T_1(^3B_1)$ "locally"-excited state character (Fig. 6). Furthermore, the $T_l(8^3A_1) \leftarrow T_1(^3B_1)$ excitation in the visible region is charge-transfer in the $D^+ \rightarrow A^-$ direction, and should therefore move to longer wavelengths (lower energy) upon increasing solvent polarity as indicated by the relative dipole moments and solvation energies given in Table 2. According to the calculated relative dipole moments
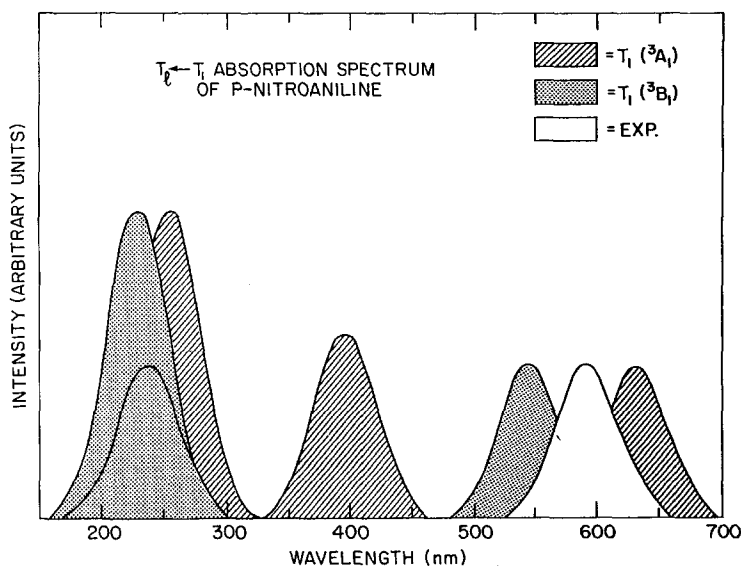

Fig. 6. A comparison of the experimental (Ref. [7]) and calculated $T_l \leftarrow T_1$ absorption spectra of PNA assuming a $^3B_1$ and $^3A_1$ T_1 character. The calculated spectra have been normalized separately so that the respective long wavelength excitation intensity corresponds with experiment

the $T_l(8^3A_1) \leftarrow T_1(^3A_1)$ excitation, also occurring in the visible region, is also expected to be red-shifted by polar solvents. This excitation involves a slight charge-transfer ($<0.05e$) from both donor and acceptor groups to the aromatic moiety and is predicted on the basis of solvation energy differences to undergo a modest blue-shift upon increasing solvent polarity. While not including specific (local) solute-solvent interactions suggested by the Jano solvation model [16, 52] our supermolecule results [16] (see also the caption to Table 2) parallels the shift obtained on the basis of dipole moment differences. The only other apparent distinction between the two cases which may be ammenable to experimental resolution, apart from the several relatively intense $T_l \leftarrow T_1(^3A_1)$ excitations in the infrared (Table 2), is the large difference in the absolute values of the $T_l \leftarrow T_1$ oscillator strengths. However, in each case the more intense $T_l \leftarrow T_1$ excitation at ~5.0 eV is approximately an order of magnitude greater than the visible excitation. This latter relationship precludes a T_1 state characterization based solely on transition intensity differences between these relatively low-lying states.

Criterion 2 of Wolleben and Testa [7] only establishes that T_1 is more strongly coupled to S_0 in PNA than in aniline, and is, therefore, not inconsistent with a $T_1(^3B_1)$ assignment. Lim and Chakrabarti [53] have established an in-plane phosphorescence for aniline (strongly suggesting a non-planar geometry) and postulated charge-transfer contributions to the phosphorescence lifetime by noting that in cases of non-planarity $\langle S_k(\pi^* \leftarrow \pi) | H' | T_1(\pi^* \leftarrow \pi) \rangle \neq 0$. C_{2v} symmetry and the out-of-plane phosphorescence of PNA, however, excludes the direct interaction of such states via the spin–orbit coupling matrix elements [49, 50]. Therefore, a comparison of the phosphorescence lifetime of aniline and PNA as a direct indication of T_1 state character is misleading; i.e., such differences may be more indicative of a different spin–orbit coupling scheme rather than relative T_1 state charge-transfer behavior.

Observation 3 of Wolleben and Testa [7] appears somewhat more definitive in terms of assigning the T_1 state of PNA (DMPNA) as either $T_1(^3B_1)$ or $T_1(^3A_1)$. The high quantum yield for photoreduction of NB in fluid polar media has commonly been attributed to a T_1 state derived from n orbital excitation from the oxygen atoms to the carbon π^*-orbital framework; i.e., charge-transfer in the $D^+ \leftarrow A^-$ direction imparts a radical character to the oxygen centers which is responsible for the high chemical reactivity [46, 54]. As we have pointed out (Table 3) the calculated $T_1(^3B_1)\pi^* \leftarrow n(\pi)$ state imparts a significantly greater

Table 3. NO_2 group atomic charge densities relative to S_0 for the indicated excitations of PNA. $^3B_1(\pi^* \leftarrow n(\pi))$ excitation corresponds to $\Delta q(NO_2) = -0.527e$. Although the $^3A_1(\pi^* \leftarrow \pi)$ $D^+ \rightarrow A^-$ excitation exhibits a relatively small degree of charge-transfer behavior, due to a difference in configuration interaction the corresponding singlet excitation yields $\Delta q(NO_2) = 0.595e$

	$^3B_1(\pi^* \leftarrow n(\pi))$	$^3A_1(\pi^* \leftarrow \pi)$	$^3A_2(\pi^* \leftarrow n(\sigma))$	$^3B_2(\pi^* \leftarrow n(\sigma))$
Δq(OXY)	−0.385	0.081	−0.318	−0.240
Δq(N)	0.243	0.219	0.236	0.255

radical character to the electronic structure than either low-lying $\pi^* \leftarrow n(\sigma)$ excitation [55]! Since the corresponding states of interest of *unperturbed* NB and PNA (DMPNA) yield similar intramolecular charge-transfer character the large decrease in the photoreduction quantum yield in going from NB to PNA appears consistent only with the $T_1(^3A_1)$ assignment for PNA as concluded by Wolleben and Testa [7]. In the strongly polar solvent in which the photoreduction experiments were carried out it is expected that level reversal between the closely-spaced strongly charge-transfer $^3A_1$ state and the considerably less polar $^3B_1$ state of PNA can be easily achieved [56]. We have, in fact, achieved such level crossing computationally for PNA using PP integrals by applying appropriate static perturbations to simulate solvent reaction field effects (see the caption to Table 2). In line with the $^3A_1$ and $^3B_1$ polarizations relative to S_0, level crossing occurred through a stabilization of $^3A_1$ and a concomitant destabilization of $^3B_1$. Due to the large energy differences between the $^3B_1$ and $^3A_1$ levels obtained using NM integrals similar supermolecule computations using NM integrals failed to produce level crossing. The magnitude of charge-transfer of the $^3A_1$ state of NB may be insufficient, owing to the absence of a donor group to provide a reaction field of sufficient strength to yield level crossing between $^3A_1/^3B_1$ in polar media.

3.4. The T_1 State of Nitrobenzene in Polar Solvents

While the above analysis provides compelling arguments that at least in polar solvents the T_1 state of PNA and DMPNA is the intramolecular $D^+ \rightarrow A^-$ charge-transfer state, neither the $^3A_1$ or $^3B_1 T_1$ assignment appears sufficient to rationalize the anomalous luminescence properties of NB under similar conditions. In addition to the probable lack of phosphorescence in NB, which is difficult to justify in terms of the calculated ordering of states (Table 1) coupled with solvent reaction field theory [57], the low-lying $\pi^* \leftarrow n(\sigma)$ singlet absorption appears to violate the "characteristic" blue-shift behavior expected for such transitions in going from non-polar to polar solvents [3, 58, 59]. Similar singlet manifold behavior in PNA and DMPNA is undoubtably masked in going to polar solvents due to the concomitant stabilization and large oscillator strength of the $^1A_1(\pi^* \leftarrow \pi)$ excitation. Wiberg [60] has suggested a specific interaction between NB and hydroxylic solvents, H_2O for example. Although it is well known that the CNDO/S technique is inadequate to achieve geometry optimization based on total energy considerations, we nevertheless performed cursory supermolecule computations on NB perturbed by a single H_2O molecule, Fig. 7. We find that as H_2O approaches the NO_2-group in the NB π-plane the p_z-orbital largely localized on the NB oxygen atoms can be strongly destabilized concomitant with a significant stabilization of the LUMO NO_2-orbital. The destabilization of the indicated $n(\sigma)p_z$-orbital for a separation of $R_{H-O} = 1.5$ Å is more than sufficient to induce level crossing in the triplet manifold yielding $T_1(^3B_2)$ in accord with the intuitive arguments of McGlynn and co-workers [3, 48]. Although additional computation is obviously required to render the solute-solvent interactions on a quantitative basis, the scheme given in Fig. 7
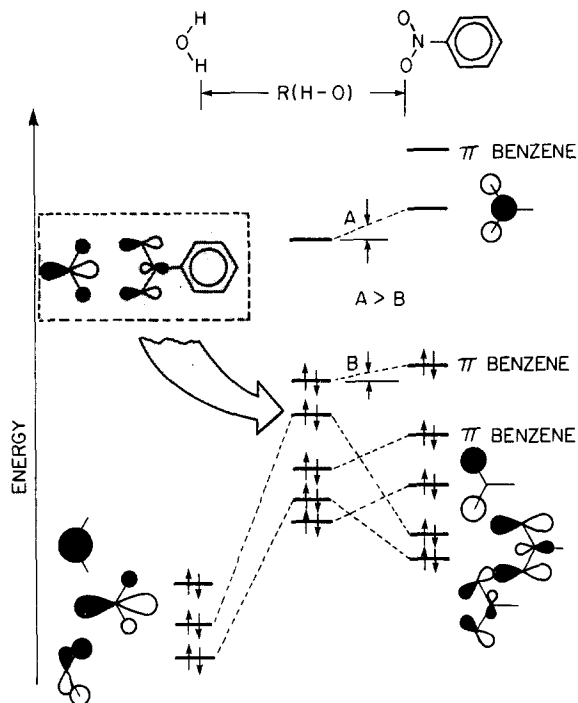
Fig. 7. The orbital correlation diagram for NB:H_2O supermolecule interaction, R(H–O) = 1.5 Å, as described in the text

appears to be a reasonable means of not only selectively stabilizing the appropriate $\pi^* \leftarrow n(\sigma)$ singlet and triplet states by microscopic or specific solvent interactions, but to stabilize the $D^+ \rightarrow A^- \pi^* \leftarrow \pi$ excitation through macroscopic or non-specific solvent effects as well [60]. It is easily rationalized that while similar interactions also stabilize the $^3B_2(\pi^* \leftarrow n(\sigma))$ excitation of PNA and DMPNA, the dipole moment of the charge-transfer state is sufficiently large due to the donor group to prohibit $^3B_2/^3A_1$ level crossing.

A $T_1(^3B_2)$ character implies an in-plane x- and/or z-axis polarized phosphorescence with matrix elements [49–51]:

$$
\begin{array}{ll}
\text{I} & \langle S_k(B_1)|H_z'(A_2)|T_1(B_2)\rangle\langle S_0(A_1)|r_x(B_1)|S_k(B_1)\rangle \\
x & \\
\text{II} & \langle T_l(A_2)|H_z'(A_2)|S_0(A_1)\rangle\langle T_l(A_2)|r_x(B_1)|T_1(B_2)\rangle \\
^3B_2: & \\
\text{I} & \langle S_k(A_1)|H_x'(B_2)|T_1(B_2)\rangle\langle S_0(A_1)|r_z(A_1)|S_k(A_1)\rangle \\
z & \\
\text{II} & \langle T_l(B_2)|H_x'(B_2)|S_0(A_1)\rangle\langle T_l(B_2)|r_z(A_1)|T_1(B_2)\rangle
\end{array}
$$

Our NB:H_2O supermolecule results yield seven $S_k \leftarrow S_0$ dipole allowed excitations below 9.0 eV with $f/\Delta E(S_k \leftarrow S_0) \sim 7.0 \times 10^{-3} \rightarrow 2.0 \times 10^{-1}$. Mechanism I will, therefore, yield a phosphorescence lifetime orders of magnitude smaller than derived from the $\pi^* \leftarrow \pi$ triplet states of interest [61, 62]. Mechanism II

provides negligible $T_1 - S_0$ coupling, relative to Mechanism I, for both x- and z-axis polarization. In addition to the reduced T_1 radiative lifetime, the suggested $^3B_2/^3A_1$ level crossing is expected to dramatically enhance inherent radiationless depletion of T_1 [63]. Furthermore, direct coupling with solvent molecules as indicated in Fig. 7, for example, is known to provide additional and efficient radiationless decay channels for depletion of T_1 through intermolecular vibronic interactions [61]. These arguments are in accord with the results of Hurley and Testa who measured a T_1 radiationless decay constant for NB of $\sim 10^9\ \text{sec}^{-1}$ [47].

4. Summary and Conclusions

This study has demonstrated that the nature of the lowest energy triplet state of the nitroaromatics nitrobenzene, p-nitroaniline and N,N-dimethyl-p-nitroaniline can be rationalized on the basis of comparisons between CNDO/S-CI computation and available experimental results.

Specifically, we conclude that the T_1 state of *unperturbed* NB, PNA and DMPNA are derived from excitation out of the non-bonding orbital localized on the oxygen atoms parallel to the molecular π-plane to the antibonding acceptor π^*-orbitals localized on the nitro group. Our computations reveal that this state is only slightly lower in energy than the highly polar $D^+ \to A^-$ intramolecular $\pi^* \leftarrow \pi$ triplet, which in the case of PNA and DMPNA is undoubtably stabilized below the less polar "localized"-excitation by interactions with polar media. This level reversal in polar solvents is consistent with the observed phosphorescence polarization and lifetime, dramatic reduction in the photoreduction quantum yield in going from NB to PNA, and the $T_n \leftarrow T_1$ absorption spectrum.

Also, we have demonstrated by supermolecule computations that direct interaction of the NB oxygen $n(\sigma)$-orbitals with solvent molecules can stabilize the $\pi^* \leftarrow n(\sigma)$ triplets below those of $\pi^* \leftarrow \pi$ character. This level reversal in the case of NB appears sufficient to rationalize: (1) the anomalous behavior of the $\pi^* \leftarrow n(\sigma)$ excitation in polar solvents, (2) the efficient radiationless depletion of T_1 through direct solvent coupling, and therefore the absence of a $T_n \leftarrow T_1$ absorption, and (3) the large photoreduction quantum yield relative to PNA.

References and Notes

1. Khalil, O. S., Meeks, J. L., McGlynn, S. P.: J. Am. Chem. Soc. **95**, 5876 (1973)
2. Khalil, O. S., Seliskar, C. J., McGlynn, S. P.: J. Chem. Phys. **58**, 1607 (1973)
3. Seliskar, C. J., Khalil, O. S., McGlynn, S. P.: Excited states, Vol. 1, p. 231–294, Lim, E. C., Ed. New York: Academic Press, 1974.
4. Khalil, O. S., Seliskar, C. J., McGlynn, S. P.: J. Mol. Spect. **70**, 74 (1978)
5. Carsey, T. P., Findley, G. L., McGlynn, S. P.: J. Am. Chem. Soc. **101**, 4502 (1979)

6. Findley, G. L., Carsey, T. P., McGlynn, S. P.: J. Am. Chem. Soc. **101**, 4511 (1979).
7. Wolleben, J., Testa, A. C.: J. Phys. Chem. **81**, 429 (1977)
8. Bigelow, R. W.: J. Chem. Phys. **73**, 3864 (1980)
9. Pignataro, S., Distefano, G.: J. Elect. Spect. Rel. Phenom. **2**, 171 (1973)
10. Pignataro, S., DiMarino, R., Distefano, G.: J. Elect. Spect. Rel. Phenom. **4**, 90 (1974)
11. Pignataro, S., Distefano, G.: Z. Naturforsch. **30A**, 815 (1975)
12. Tsuchiya, S., Seno, M.: Chem. Phys. Letters **54**, 132 (1978)
13. Domcke, W., Cederbaum, L. S., Schirmer, J., von Niessen, W.: Chem. Phys. **39**, 149 (1979)
14. Banna, M. S.: Chem. Phys. **45**, 383 (1980)
15. Bigelow, R. W., Freund, H.-J.: Chem. Phys. Letters **77**, 261 (1981)
16. Freund, H.-J., Bigelow, R. W.: Chem. Phys. **55**, 407 (1981)
17. Morrell, J. A., Albrecht, A. C.: Chem. Phys. Letters **64**, 46 (1979)
18. Lalama, S. J., Garito, A. F.: Phys. Rev. **A20**, 1179 (1979)
19. Levine, B. F.: J. Chem. Phys. **63**, 115 (1975)
20. Levine, B. F.: Chem. Phys. Letters **37**, 516 (1976)
21. Oudar, J. L., Chemla, D. S.: J. Chem. Phys. **66**, 2664 (1977)
22. Oudar, J. L.: J. Chem. Phys. **67**, 446 (1977)
23. Levine, B. F., Bethea, C. G.: J. Chem. Phys. **69**, 5240 (1978)
24. Nishimoto, K., Mataga, N.: Z. Phys. Chem. (Frankfurt am Main) **12**, 335 (1957)
25. Smith, H. E., Cozart, W. I., dePaulis, T., Chen, F. M.: J. Am. Chem. Soc. **101**, 5186 (1979). These workers argue in favor of low-lying PNA $\pi^* \leftarrow n(\sigma)$ singlet excitations based on a comparison of independent CNDO/S-CI results with the PNA crystal spectrum
26. In this regard our results parallel those of Plotnikov, V. G. and Komarov, V. M.: Spect. Letters **9**, 265 (1976). It should be noted, however, that Plotnikov and Komarov do not mention a $D^+ \rightarrow A^-$ triplet $\pi^* \leftarrow \pi$ intramolecular charge-transfer excitation, although their work explicitly yields such character for the S_1 state
27. As discussed in the text the T_1 state we define for the unperturbed molecules in this study is derived from a π-orbital lone-pair completely localized on the oxygen centers. According to Sidman, J. W.: Chem. Rev. **58**, 689 (1958), for example, any orbital largely localized in space can be properly classified as lone-pair (n), where n may be either parallel to, $n(\pi)$, or orthogonal to, $n(\sigma)$, the main π-electron framework. We emphasize this point here because it appears that in the literature such an n-orbital distinction, particularly in regard to the nitroanilines, has often been reserved for $n(\sigma)$-type orbitals (see Refs [5] and [24], for example). For simplicity, however, we also reserve the n classification primarily for $n(\sigma)$-type orbitals and explicitly indicate the lone-pair nature of the oxygen π-orbital in question as $n(\pi)$ whenever failure to do so would cause some confusion
28. Parr, R. G.: J. Chem. Phys. **20**, 1499 (1952)
29. Pariser, R., Parr, R. G.: J. Chem. Phys. **21**, 767 (1953)
30. DelBene, J., Jaffé, H. H.: J. Chem. Phys. **48**, 1807, 4050 (1968); **49**, 1221 (1968); **50**, 1126 (1969)
31. Ellis, R. L., Kuehnlenz, G., Jaffé, H. H.: Theoret. Chim. Acta (Berl.) **26**, 131 (1972)
32. Dick, B., Hohlneicher, G.: Theoret. Chim. Acta (Berl.) **53**, 221 (1979)
33. Dick, B.: Chem. Phys., to be submitted for publication
34. Pople, J. A., Beveridge, D. L.: Approximate molecular orbital theory, p. 111. New York: McGraw-Hill, 1970
35. Jacques, P., Faure, J., Chalvet, O., Jaffé, H. H.: J. Phys. Chem. **85**, 473 (1981)
36. Bertinelli, F., Polmieri, P., Brillante, A., Taliani, C.: Chem. Phys. **25**, 333 (1977)
37. Davis, L. P., Guidry, R. M.: Aust. J. Chem. **32**, 1369 (1979)
38. Masmanidis, C. A., Jaffé, H. H., Ellis, R. L.: J. Phys. Chem. **79**, 2052 (1975).
39. Chang, H. M., Jaffé, H. H.: Chem. Phys. Letters **23**, 146 (1973)
40. Koutecky, J.: J. Chem. Phys. **47**, 1501 (1967)
41. For a recent discussion of this problem with emphasis on the CNDO/S-CI method see Ref. [32] and references contained therein
42. Roothaan, C. C. J.: Rev. Mod. Phys. **23**, 69 (1951)
43. Oikawa, S., Tsuda, M., Ueno, N., Sugita, K.: Chem. Phys. Letters **74**, 379 (1980)
44. Ito, H., I'Haya, Y.: Bull. Chem. Soc. Japan **49**, 940 (1976)

45. Suzuki, H.: Electronic absorption spectra and geometry of organic molecules, pp. 190–192; 430. New York: Academic Press, 1967
46. Lewis, G. N., Kasha, M.: J. Am. Chem. Soc. **66**, 2100 (1944)
47. Hurley, R., Testa, A. C.: J. Am. Chem. Soc. **90**, 1949 (1968)
48. Khalil, O. S., Bach, H. G., McGlynn, S. P.: J. Mol. Spect. **35**, 455 (1970)
49. McGlynn, S. P., Azumi, T., Kinoshita, M.: Molecular spectroscopy of the triplet state. New Jersey: Prentice-Hall, 1969
50. Hochstrasser, R. M.: Molecular aspects of symmetry. New York: Benjamin, 1966
51. Wild, U.P.: Topics in Current Chem. **55**, 1 (1975)
52. Jano, I.: Compt. Rend. Acad. Sci. Paris **261**, 103 (1965)
53. Lim, E. C., Chakrabarti, S. K.: Chem. Phys. Letters **1**, 28 (1967)
54. Döpp, D.: Topics in Current Chem. **55**, 49 (1975)
55. Plotnikov and Kamarov (Ref. [26]) also emphasized that such a $T_1(^3B_1)$ assignment corresponds to a state of high chemical reactivity
56. Khalil, O. S., McGlynn, S. P.: J. Luminescence **11**, 185 (1975/76)
57. Ledger, M. B., Suppan, P.: Spectrochim. Acta **23A**, 641 (1967)
58. Nagakura, S., Kojima, M., Maruyama, Y.: J. Mol. Spectros. **13**, 174 (1964)
59. Vidal, B., Murrell, J. N.: Chem. Phys. Letters **31**, 46 (1975)
60. Wiberg, K. B.: Physical organic chemistry, p. 189. New York: Wiley, 1964
61. Ref. [49], pp. 246–247
62. Vanquickenborne, L., McGlynn, S. P.: J. Chem. Phys. **43**, 4755 (1966)
63. Mataga, N., Kubota, T.: Molecular interactions and electronic spectra. New York: Marcel Dekker, Inc., 1970